

# High-resolution comparison of sediment dynamics under different forcing conditions in the bottom boundary layer of a shallow, micro-tidal estuary

Ho Kyung Ha<sup>1,2</sup> and Kyeong Park<sup>2</sup>

Received 6 January 2012; revised 19 April 2012; accepted 11 May 2012; published 26 June 2012.

[1] Data for high-resolution profiles of current velocity and suspended sediment concentration (SSC) were collected in bottom boundary layer (BBL) of Mobile Bay, Alabama. The data were used to study the vertical and temporal variability in SSC under various forcing conditions of tide, wind and freshwater discharge. During the winter stormy season, the background SSC was low ( $0.015\text{--}0.03\text{ g l}^{-1}$ ). An episodic storm-induced erosion/resuspension was responsible for the short-lasting high SSC in BBL. During the spring flooding period, the background SSC was relatively high ( $0.04\text{--}0.07\text{ g l}^{-1}$ ) likely due to the large amount of suspended sediment from the fluvial input and bed softening, and the contribution of wind forcing to sediment resuspension was somewhat enhanced by the destratification in BBL. When the freshwater discharge was extremely high ( $>5000\text{ m}^3\text{ s}^{-1}$ ), the entire water column in shallow areas of the Bay was influenced by freshwater input. Therefore, the thermohaline anomaly's contribution to the stratification considerably weakened, while the SSC's contribution strengthened. When the freshwater discharge was relatively low ( $<5000\text{ m}^3\text{ s}^{-1}$ ), a critical wind stress for sediment erosion ( $0.08\text{--}0.1\text{ Pa}$ ) was observed to abruptly increase the SSC. Despite a micro-tidal regime, Mobile Bay exhibited the cyclic erosion and deposition pattern induced by the tidal acceleration and deceleration.

**Citation:** Ha, H. K., and K. Park (2012), High-resolution comparison of sediment dynamics under different forcing conditions in the bottom boundary layer of a shallow, micro-tidal estuary, *J. Geophys. Res.*, 117, C06020, doi:10.1029/2012JC007878.

## 1. Introduction

[2] Water clarity/turbidity is a basic measure of water quality. Clarity influences public's perception of water and their willingness to utilize it. Turbidity is important in affecting the primary production by regulating light penetration [Lohrenz *et al.*, 1999] and toxic contaminants because of their affinity to sediment [Menon *et al.*, 1998]. Turbidity has a coherent relationship with suspended sediment concentration (SSC), which is primarily governed by erosion/resuspension and deposition of sediment at water-sediment interface. Resuspension itself plays an important role in productivity dynamics of water column and benthic sediment in shallow estuaries [Shaffer and Sullivan, 1988; de Jonge and van Beusekom, 1995; MacIntyre and Cullen, 1996]. Resuspended organic matter may exert an enhanced demand on oxygen level in shallow environments [Wainright

and Hopkinson, 1997]. Deposition may cause smothering of benthic aquatic organisms and clogging of water intakes, and may request a high cost for maintenance of navigational channels [Winterwerp and van Kesteren, 2004].

[3] In sediment dynamics, erosion/resuspension and deposition are determined by interplay between hydrodynamic conditions (e.g., current velocity) and sediment properties (e.g., concentration and size) in bottom boundary layer (BBL). Because both current velocity and SSC exhibit large vertical gradient and temporal variability in BBL, their measurements require high spatial and temporal resolution. Mooring of single-point current meters inside BBL is not ideal because their intrusive nature disturbs flow structure in BBL, and they also fail to provide adequate vertical resolution (on the order of millimeters to centimeters). Various methods have been employed to measure SSC [Wren *et al.*, 2000]. Simply, direct water sampling is the most straightforward method and is considered as a standard to get the true SSC against other methods that require calibration. However, its time- and labor-intensive procedure in field and laboratory makes it impossible to meet adequate spatial and temporal resolution simultaneously. An optical instrument such as an optical backscattering sensor is a good alternative to measure SSC at a single point, and its response is well studied for a wide range of SSC [Kineke and Sternberg, 1992; Sutherland *et al.*, 2000; Downing, 2006]. Being

<sup>1</sup>Korea Polar Research Institute, Korea Ocean Research and Development Institute, Incheon, South Korea.

<sup>2</sup>Dauphin Island Sea Lab, Department of Marine Sciences, University of South Alabama, Dauphin Island, Alabama, USA.

Corresponding author: H. K. Ha, Korea Polar Research Institute, Incheon 406-840, South Korea. (ha@kopri.re.kr)

©2012. American Geophysical Union. All Rights Reserved.  
10.1029/2012JC007878

intrusive, however, it also disturbs flow structure and hardly provides adequate vertical resolution in BBL. With these manifold requests by sediment dynamics community, the high-frequency acoustic instruments have been spotlighted as a non-intrusive method to study the BBL processes [Thorne and Hanes, 2002]. Most recently, a pulse-coherent acoustic Doppler current profiler (PC-ADCP) has emerged with high-resolution profiling capability with an attainable spatial resolution of 1–2 cm [RD Instruments, 2002]. A PC-ADCP, hence, has a merit to simultaneously measure hydrodynamic and sedimentary conditions in BBL with fine enough a resolution and without disturbing flow structure and sediment distribution [Lacy and Sherwood, 2004; Ha et al., 2011].

[4] Many estuaries along the northern Gulf of Mexico (NGOM) possess several common attributes: shallow and wide bathymetry with deep and narrow ship channels, diurnal tides with a micro-tidal range, relatively large river discharge, high turbidity and exchange with the NGOM via relatively narrow passes [Schroeder and Wiseman, 1999]. In the shallow, micro-tidal estuaries, wind becomes an important factor invoking sediment resuspension, which would affect large portion of, if not entire, water column. Importance of resuspension on various biological/ecological processes in water column and benthic sediment of the shallow NGOM estuaries has been suggested and discussed [e.g., MacIntyre and Cullen, 1996; Stutes et al., 2006; Pinckney and Lee, 2008], but the details of erosion/resuspension process itself have not been studied with high vertical and temporal resolution.

[5] To improve the understanding of sediment behavior in BBL under specific forcing conditions, we carried out a mooring study in Mobile Bay, as a case system for the NGOM estuaries. Main focus was to compare different periods dominated by each of tide, wind and river discharge. By utilizing the PC-ADCP's advantages over other traditional methods, this study attempted: (1) to obtain high-resolution profiles of current velocity and SSC in BBL of the middle of shallow Mobile Bay, and (2) to reveal the relationships between forcing functions (tide, wind and freshwater discharge) and sediment behavior (erosion/resuspension and deposition) in the context of BBL dynamics.

## 2. Study Area

[6] Mobile Bay is an estuary where the freshwater from the sixth largest drainage basin area in the U.S. [Johnson et al., 2002] mixes with the salt water from the NGOM (Figure 1). The Bay has a triangular-shaped morphology, approximately 50 km long and 39 km cross at its widest point [Mobile Bay National Estuary Program (MBNEP), 2008]. The Bay has a regularly-dredged ship channel along the north-south axis that connects the port of Mobile to the NGOM. The channel is approximately 12–14 m deep and 120 m wide to accommodate the large ship traffics. Except the channel, the Bay is very shallow with an average depth of approximately 3 m [Schroeder and Wiseman, 1986].

[7] Astronomical tide is predominantly diurnal with the tropic-equatorial cycle (period of 13.66 days) and tidal range varies between <0.1 m during equatorial tides and 0.8 m during tropic tides. The micro-tidal amplitude would produce relatively weak tidal currents within the Bay, but

maximum tidal currents at the narrow Bay mouth were reported to reach up to about  $1.0 \text{ m s}^{-1}$  [Stumpf et al., 1993].

[8] The principal source of freshwater discharge ( $Q_F$ ) is two major river systems, the Alabama-Coosa-Tallapoosa River Basin and the Warrior-Tombigbee River Basin [MBNEP, 2008], which combine to account for about 95% of total freshwater input into the Bay [Schroeder, 1979]. The annual discharge is the fourth largest in the U.S. [Stumpf et al., 1993]. The long-term (1976–2009) mean daily discharge is  $1715 \text{ m}^3 \text{ s}^{-1}$ , and the 25th, 50th, 75th and 90th percentiles are 446, 926, 2251 and  $4549 \text{ m}^3 \text{ s}^{-1}$ , respectively. There is a distinct seasonality in the river discharge with maxima occurring in late winter and early spring and minima occurring in late summer and fall. The buoyant plume of river-driven terrigenous sediment has been frequently observed by satellite images [Stumpf et al., 1993; Zhao et al., 2011]. Especially during the extreme flooding events, large volume of sediments eroded from the watershed enters the Bay, and then is delivered to the inner shelf.

[9] Wind is an important forcing agent that controls vertical mixing and related sediment transport in shallow Mobile Bay. Wind shows a distinct seasonal variation, with southerly winds dominating in spring and summer and stronger northerly winds dominating in fall and winter [Schroeder and Wiseman, 1986; Noble et al., 1996]. The episodic expansion of cold fronts from the north would trigger vigorous turbulent mixing [Zhao and Chen, 2008] while reducing the temperature in air and surface water. During the hurricane seasons, the tropical storms would stir up the entire water column and severely erode the bottom sediment, resulting in highly turbid conditions [Park et al., 2007b].

## 3. Data Collection and Processing

### 3.1. Mooring

[10] A mooring site ( $30^\circ 24' 51'' \text{N}$ ,  $88^\circ 03' 55'' \text{W}$ ), with a mean depth of 3.5 m, is located in the Whitehouse Reef on the western side of the ship channel (Figure 1). The bottom sediment at this site is muddy, and the mean grain size of suspended sediment is about  $9.8 \mu\text{m}$  [Ha et al., 2011]. Two deployments were conducted to measure the current, tide and SSC: one for the winter stormy season (November 14 to December 16, 2008) and the other for the spring flooding period (March 24 to April 23, 2009). The mooring package consisted of an ADCP (RDI WorkHorse Sentinel, 600 kHz) and multi-parameter Sondes (YSI, 6600EDS). A downward-looking ADCP was installed on a pile constructed for artificial reefs, with the transducers placed at 2 m above bed (mab). To avoid the effect of the pile on emitted acoustic beams, a 2-m horizontal extended arm was mounted on the pile. Table 1 shows the values used for setup parameters. The blanking distance was set to 0.5 m, and the bin size was chosen at 0.1 and 0.05 m for 2008 and 2009 deployments, respectively. It is acknowledged that the used bin sizes are too coarse to measure the change in thickness of fluffy layer, which can be actually less than several millimeters. However, the existence of thick fluffy layer can be identified by the interpolation of acoustic signals. In this study, therefore, we examined the near-bed BBL ( $\sim 1.5 \text{ mab}$ ) including unconsolidated, fluffy layer immediately above the consolidated sediment bed. The ADCP was operated under a 5-min burst mode to store turbulent velocities and acoustic

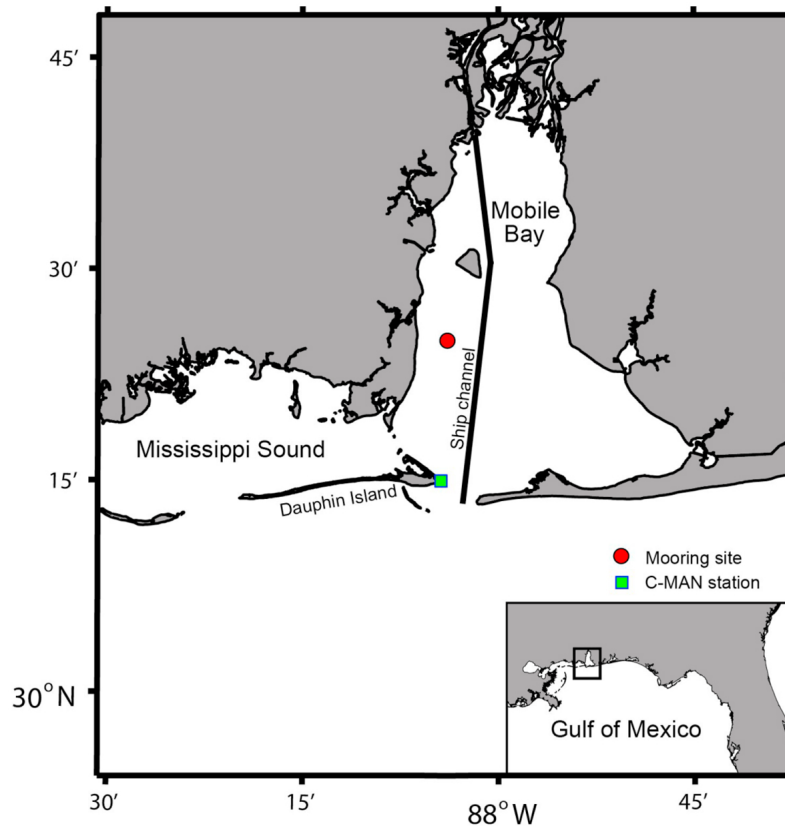


**Figure 1.** Map of study area showing the mooring site (mean depth: 3.5 m) and C-MAN station (DPIA1).

backscatter intensities at the sampling rate of 2 Hz. To attain high vertical resolution and measurement accuracy, the feature of mode 11 [RD Instruments, 2002] was selected in configuration setup. Multi-parameter Sondes were also installed at four and five levels in 2008 and 2009 surveys, respectively (Table 1). A 5-min burst mode was used to store water level, temperature, salinity and turbidity.

[11] At 1–2 week intervals, instruments were serviced and a conductivity-temperature-depth (CTD) profiler (SeaBird, SBE-25) was used to measure profiles of temperature and salinity throughout the water column. At each maintenance survey, in-situ water samples were collected through a PVC tube at the levels where YSI Sondes were deployed. Variable volumes (0.03–0.5 l) of water samples were filtered under the vacuum using pre-weighed and pre-dried 0.7- $\mu\text{m}$  glass fiber filters (GF/F). The residues on filters were oven-dried at 100°C for at least 24 h and reweighed. The SSC was determined by the weight difference divided by the volume of water filtered, which then was used to calibrate backscatter intensities from ADCP and YSI’s turbidity optic sensors. Ha *et al.* [2011] demonstrated a good correlation between backscatter signals from two sensors.

### 3.2. Suspended Sediment Concentration

[12] The simplified sonar equation by Deines [1999] was modified and used to derive the SSC profiles from ADCP’s backscatter intensities. Because the actual sensing range of the ADCP was within 1.5 mab where the bottom fluffy sediment can be actively resuspended, the contribution of suspended sediment to sound attenuation was additionally

included in the original equation of Deines [1999], which simply leads to

$$\overline{S}_v = K_c E + C', \quad (1)$$

where  $\overline{S}_v = 10 \cdot \log(SSC) - 2(\alpha_w + \alpha_s)R - 10 \cdot \log(R^2)$  is the net volume scattering corrected by subtracting the sound spreading and attenuation in the sensing range,  $E$  is echo level,  $R$  is range between transducer and measurement volume,  $\alpha_w$  and  $\alpha_s$  are sound attenuation coefficients by water and suspended sediment, respectively. At several levels where the water-based SSCs were measured, two calibration constants,  $K_c$  and  $C'$ , were determined by a linear regression [Deines, 1999; Kim and Voulgaris, 2003; Traykovski *et al.*,

**Table 1.** Setups of Deployed ADCP and YSI Sondes

|                           | Winter 2008                                    | Spring 2009                                       |
|---------------------------|--|---|
| ADCP (RDI, 600 kHz)       |  |   |
| Bin size (m)              | 0.1  | 0.05  |
| Sampling rate (Hz)        | 2  | 2   |
| Burst interval (h)        | 1  | 0.5   |
| Burst duration (min)      | 5  | 5   |
| Deployment depth (mab)    | 2  | 2   |
| Blanking distance (m)     | 0.5  | 0.5   |
| YSI Sondes (YSI, 6600EDS) |  |   |
| Sampling rate (Hz)        | 1  | 1   |
| Burst interval (h)        | 1  | 0.5   |
| Burst duration (min)      | 5  | 5   |
| Deployment depth (mab)    | 4 levels<br>(0.15, 0.5, 1 and 3 <sup>a</sup> ) | 5 levels<br>(0.15, 0.5, 1 <sup>a</sup> , 2 and 3) |

<sup>a</sup>Partially malfunctioned during the deployment.

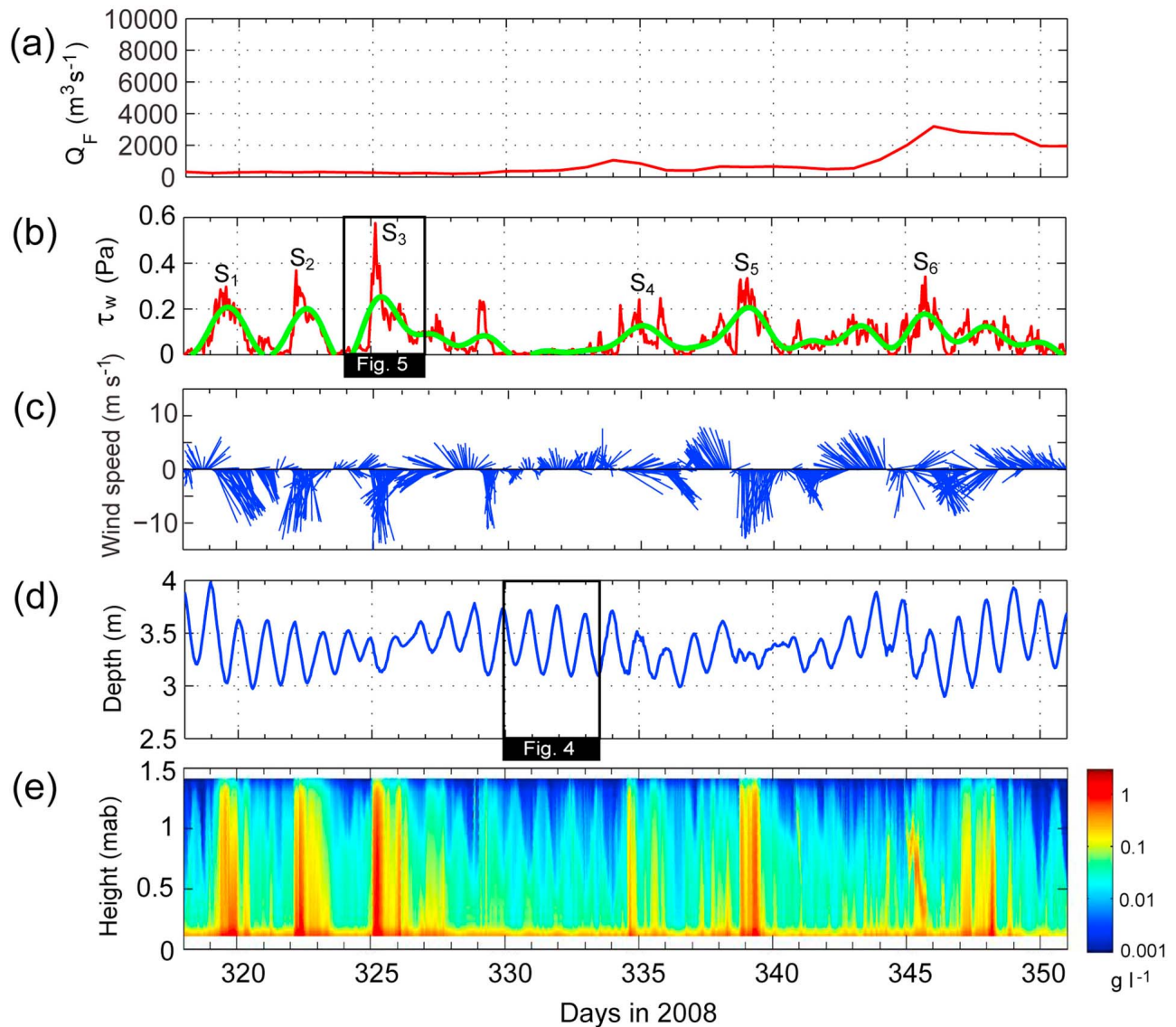


**Figure 2.** Time series from winter deployment (November 14 to December 16, 2008): (a) freshwater discharge, (b) wind stress, (c) wind, (d) water depth, and (e) ADCP-derived SSC. Thick line in Figure 2b is the low-pass filtered data.

2007; Ha *et al.*, 2011]. The detailed algorithm for converting ADCP's backscatter intensities to real SSC profiles can be found in Deines [1999], and the performance of PC-ADCP was evaluated by Ha *et al.* [2011].

[13] In the acoustic signal processing, the average of synchronous backscatter intensities collected from four transducers was used. When the maximum difference among four intensities exceeded 2 dB, as Hoitink and Hoekstra [2005] suggested, they were discarded for data quality control. This process could effectively remove undesirable noises probably produced by the existence of fish or other organisms.

### 3.3. Reynolds Stress From ADCP

[14] Three components (east, north and vertical) of flow velocity were recorded at 0.1 or 0.05 m bin intervals, and later were transformed into the beam coordinate velocities ( $u_1, u_2, u_3$  and  $u_4$ ) using a specific transformation matrix that the manufacturer calibrated to compensate for small beam

misalignments as well as measured motion parameters of pitch, roll and heading angles [RD Instruments, 2008]. In our mooring, the ADCP was firmly attached to the stable pile and the three motion parameters were almost constant during the entire deployment period. The converted four beam velocities were used to calculate the ( $x, y$ ) components of Reynolds stress ( $\tau_R$ ) using the variance technique proposed by Lohrmann *et al.* [1990] and Stacey *et al.* [1999]

$$\begin{aligned} \frac{\tau_{Rx}}{\rho} &= \overline{u'w'} = \frac{\text{var}(u_3) - \text{var}(u_4)}{4 \sin \theta \cos \theta}, \\ \frac{\tau_{Ry}}{\rho} &= \overline{v'w'} = \frac{\text{var}(u_1) - \text{var}(u_2)}{4 \sin \theta \cos \theta}, \end{aligned} \quad (2)$$

where  $\text{var}(u_i)$  indicates the variance of the velocity along the  $i$ th acoustic beam ( $u_i$ ), the overbar indicates time average, the prime indicates temporal fluctuation, and  $\theta$  is the slant angle from the vertical axis ( $20^\circ$  in this case).

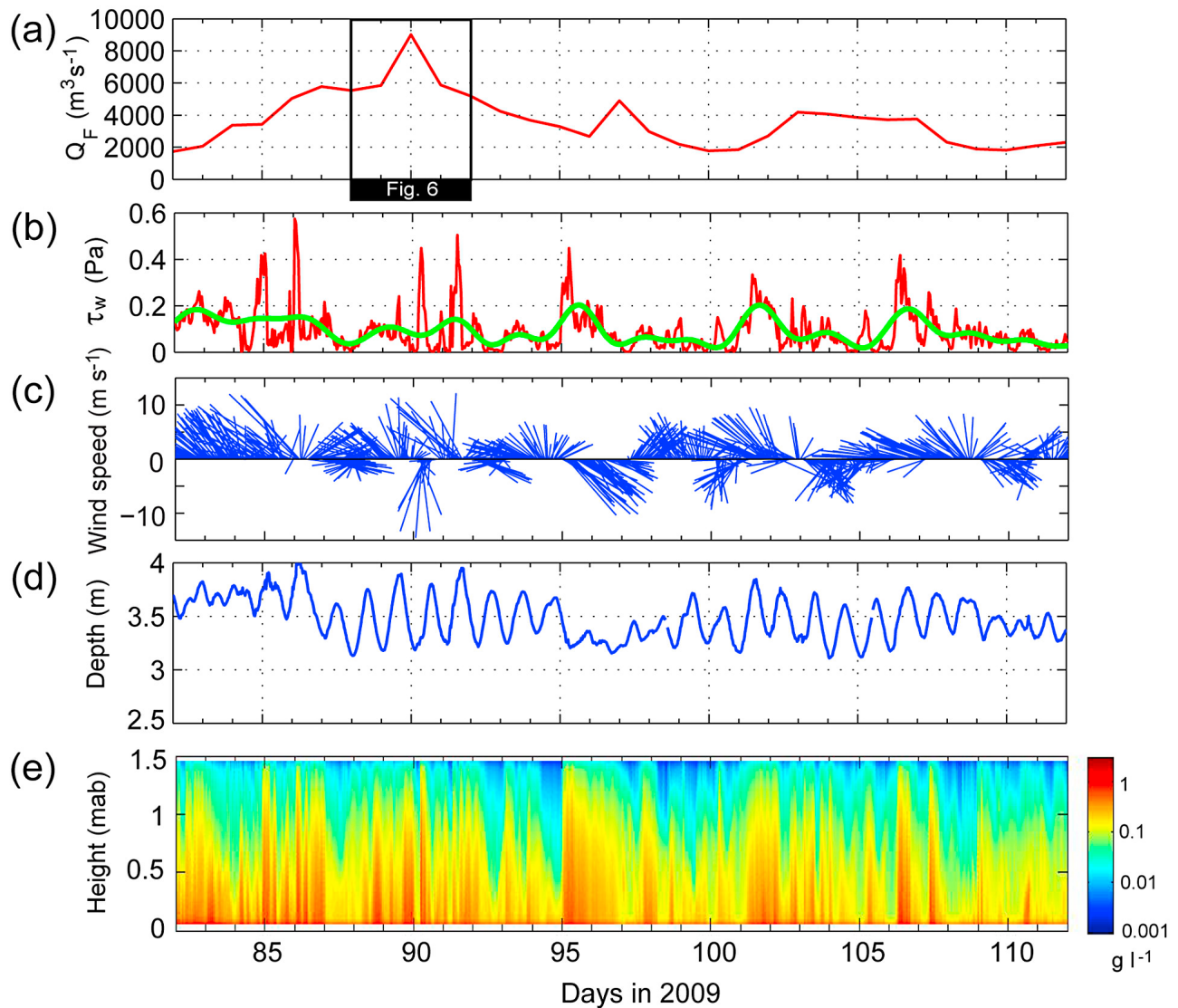


**Figure 3.** Time series from spring deployment (March 19 to April 22, 2009): (a) freshwater discharge, (b) wind stress, (c) wind, (d) water depth, and (e) ADCP-derived SSC. Thick line in Figure 3b is the low-pass filtered data.

[15] The time series of  $\tau_R$  in the near-bed bin (13th bin at 0.16–0.26 mab and 27th bin at 0.125–0.175 mab for 2008 and 2009, respectively) were extracted and used to evaluate the correlation with variations in SSC. The strongest acoustic signals off the sediment bed may produce biased velocities at the bins very close to the bottom [Gordon, 1996]. We chose the bins that were free of the effect of bottom, and thus could be a proper proxy for bed shear stress.

### 3.4. Wind and Freshwater Discharge

[16] Hourly wind data were obtained at the Coastal-Marine Automated Network (C-MAN) station, DPIA1 (Dauphin Island; 30°14'54"N, 88°04'24"W), maintained by the National Oceanic and Atmospheric Administration (NOAA)'s National Data Buoy Center (NDBC) (Figure 1). The wind stress ( $\tau_w$ ) was computed by the quadratic law given as

$$\tau_w = \rho_a C_d |W|W, \quad (3)$$

where  $\rho_a = 1.2 \text{ kg m}^{-3}$  is the air density,  $C_d$  is the drag coefficient, and  $W$  is the wind speed ( $\text{m s}^{-1}$ ).  $C_d$  which generally increases with the wind speed was estimated by following  $Wu$  [1980]. Daily freshwater discharge data from two gaging stations, Claiborne L&D (31°36'54"N, 87°33'02"W) in Alabama River and Coffeeville L&D (31°45'30"N, 88°07'45"W) in Tombigbee River, were obtained from U.S. Geological Survey. The sum of the two discharges was considered as total river discharge into Mobile Bay, following Park *et al.* [2007a].

## 4. Results

[17] Data from the winter deployment (November 14 to December 16, 2008) are presented in Figure 2. The freshwater discharge remained low until it rapidly increased to over  $3000 \text{ m}^3 \text{ s}^{-1}$  in the later part of the deployment. The average prevailing winds exhibited a seasonal northerly

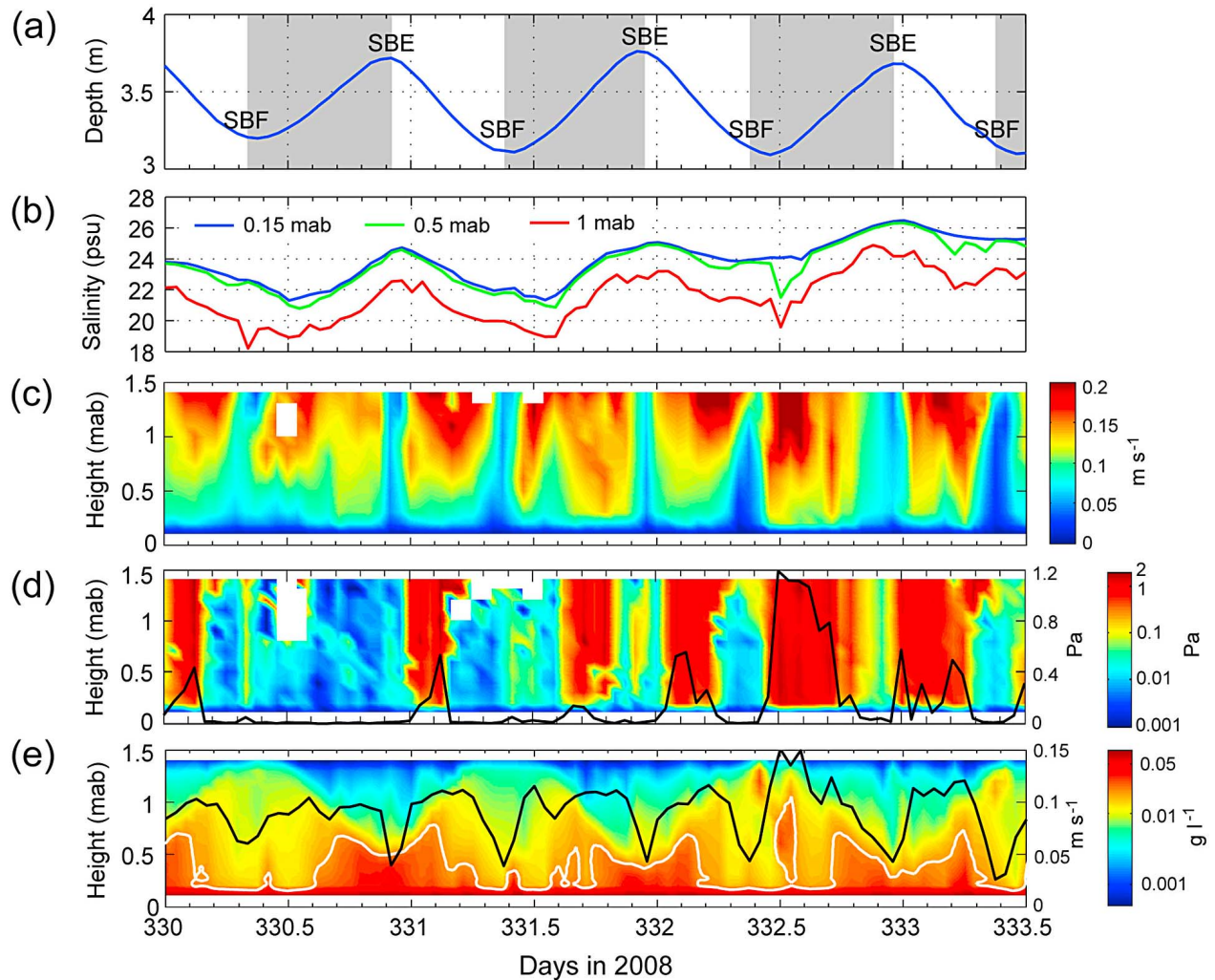


**Figure 4.** Conditions during tropic tide under fair weather conditions with low freshwater discharge and weak wind (see Figure 2d): (a) water depth, (b) salinities at three levels, (c) current speed, (d) Reynolds stress, and (e) ADCP-derived SSC. The gray and white areas in Figure 4a indicate the periods of flood and ebb, respectively. The black solid lines in Figures 4d and 4e are the Reynolds stress at the 13th bin (0.16–0.26 mab) and the BBL-averaged current speed, respectively. The white line in Figure 4e indicates  $\text{SSC} = 0.04 \text{ g l}^{-1}$ , used as the upper boundary of tide-induced high-concentration layer. White squares in Figures 4c and 4d are data discarded for quality control (see section 2).

pattern. Winter storm events associated with the southward extension of cold fronts have passed the mooring site several times ( $S_1$  to  $S_6$  in Figure 2b). During the storm passage,  $\tau_w$  sharply increased, up to 0.58 Pa on 325.2 d, and air temperature dropped abruptly by 5–15°C (not shown). Water depth showed diurnal cycles with a maximum range of about 0.8 m over a fortnightly period. The background SSC, defined as the BBL-averaged SSC under fair weather conditions, was 0.015–0.03  $\text{g l}^{-1}$ , and the peaks in SSC were always accompanied by the strong wind events.

[18] Data from the spring deployment (March 24 to April 23, 2009) are presented in Figure 3. The freshwater discharge persisted above the long-term 75th percentile ( $2251 \text{ m}^3 \text{ s}^{-1}$ ) most of the time. During 86–92 d, in particular, an extreme flooding event occurred with a peak discharge of  $9011 \text{ m}^3 \text{ s}^{-1}$ , nearly twice of the long-term 90th percentile ( $4549 \text{ m}^3 \text{ s}^{-1}$ ). The average prevailing winds were

southerly. Strong wind events occurred frequently, but their durations were shorter than those of winter storms. It is noted that strong wind events were not always accompanied by the drop in air temperature (not shown), unlike in winter season. The background SSC was relatively high (0.04–0.07  $\text{g l}^{-1}$ ), 2–3 times of winter season background level. The SSC showed a number of peaks, some of which were not associated with strong wind events.

[19] Three time periods, indicated in Figures 2 and 3, were selected and examined in more details to investigate the sediment behavior in BBL under dominant forcing conditions of tide (Figure 4), wind (Figure 5) and freshwater discharge (Figure 6).

#### 4.1. Tidal Forcing

[20] In order to clearly reveal the role of tidal currents in determining the sediment behavior in BBL, a fair weather

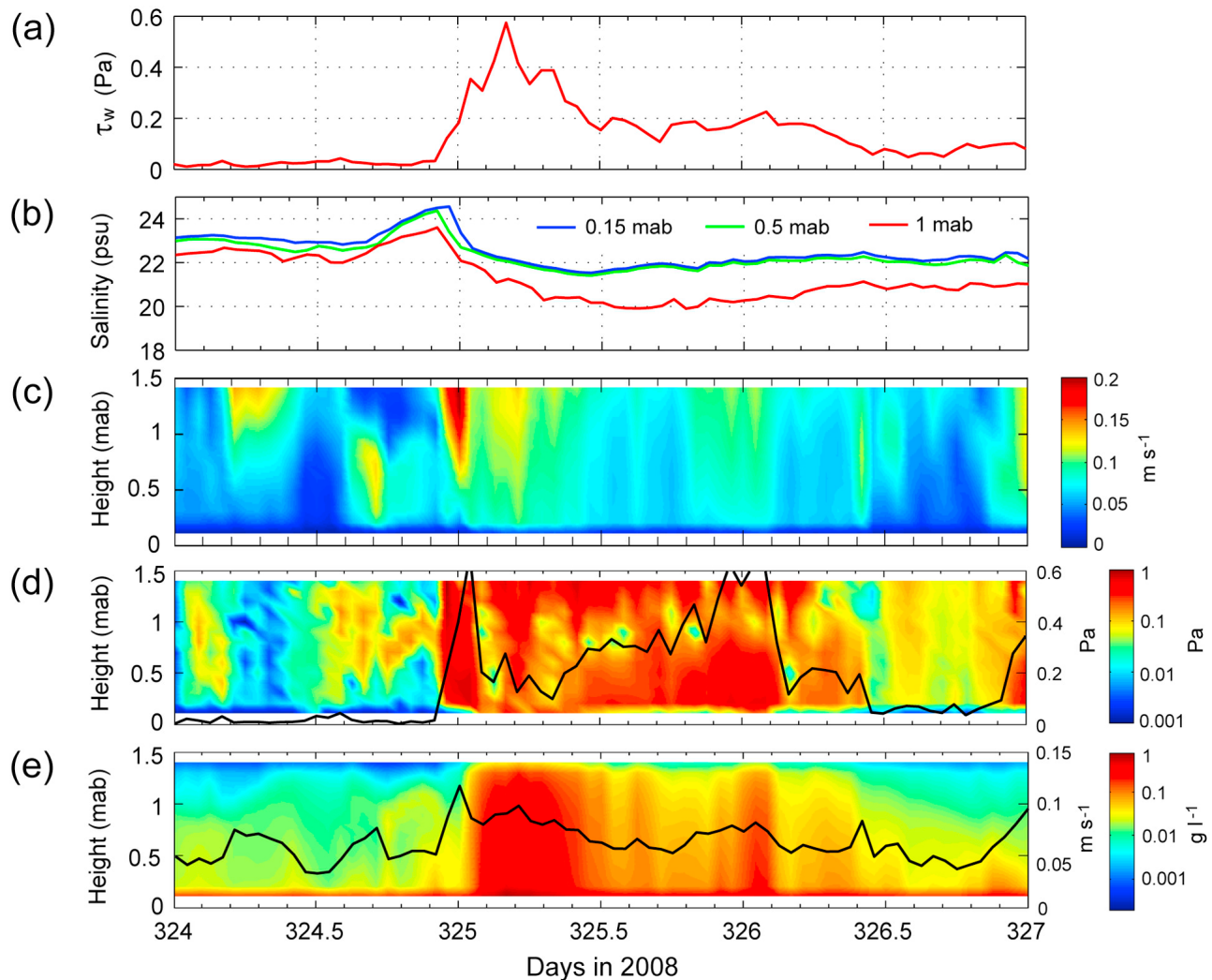


**Figure 5.** Conditions during the passage of a storm ( $S_3$  in Figure 2b): (a) wind stress, (b) salinities at three levels, (c) current speed, (d) Reynolds stress, and (e) ADCP-derived SSC. The black solid lines in Figures 5d and 5e are the Reynolds stress at the 13th bin (0.16–0.26 mab) and the BBL-averaged current speed, respectively.

condition (330–333.5 d in Figure 2d) was selectively examined in Figure 4. This time window corresponded to tropic tide with very calm wind (mean  $\tau_w = 0.01$  Pa). The mean freshwater discharge during this period was  $443.5 \text{ m}^3 \text{ s}^{-1}$ , close to the long-term 25th percentile ( $446 \text{ m}^3 \text{ s}^{-1}$ ).

[21] The water depth fluctuation was primarily due to the diurnal tide with a maximum range of approximately 0.7 m. The salinity exhibited a distinct tidal variation, ranging between 21.3–26.5 psu at 0.15 mab and 18.2–24.9 psu at 1 mab (Figure 4b). There was virtually no salinity difference between 0.15 and 0.5 mab, but large salinity gradient (4–6 psu  $\text{m}^{-1}$ ) persisted between 0.5 and 1 mab. This indicates the presence of relatively strong salinity gradient outside of the near-bed 0.5-m layer.

[22] The velocity structure during this tide-dominated period was affected by two-layer gravitational circulation, consistent with observations in other estuaries [Jay and Musiak, 1994; Sanford et al., 2001]. The height of maximum

current was lowered on flood and the opposite on ebb and the near-bottom current turned to flood sooner and to ebb later, which resulted in stronger velocity shear during ebb than during flood (Figure 4c). It is noted that relatively strong currents intermittently extended down to the near-bed layer. On 332.5 d, for example, the current speed at 0.8 mab reached  $0.2 \text{ m s}^{-1}$ . The duration of slack before flood (SBF) near the bed was longer than that of slack before ebb (SBE). The  $\tau_R$  also showed a distinct diurnal variation (Figure 4d). During the tidal accelerating phase the BBL exhibited  $\tau_R$  higher than 1 Pa with an exception of 330.5–330.7 d, whereas during the decelerating phase the  $\tau_R$  quickly decreased. The near-bed  $\tau_R$  showed the periodic presence of strong stress (solid line in Figure 4d), which is clearly related to variation in SSC profiles (Figure 4e).

[23] The tidal signal on SSC in BBL was clearly detected. The current speed (Figure 4c) matched well with the thickness of high-concentration layer (white line in Figure 4e).

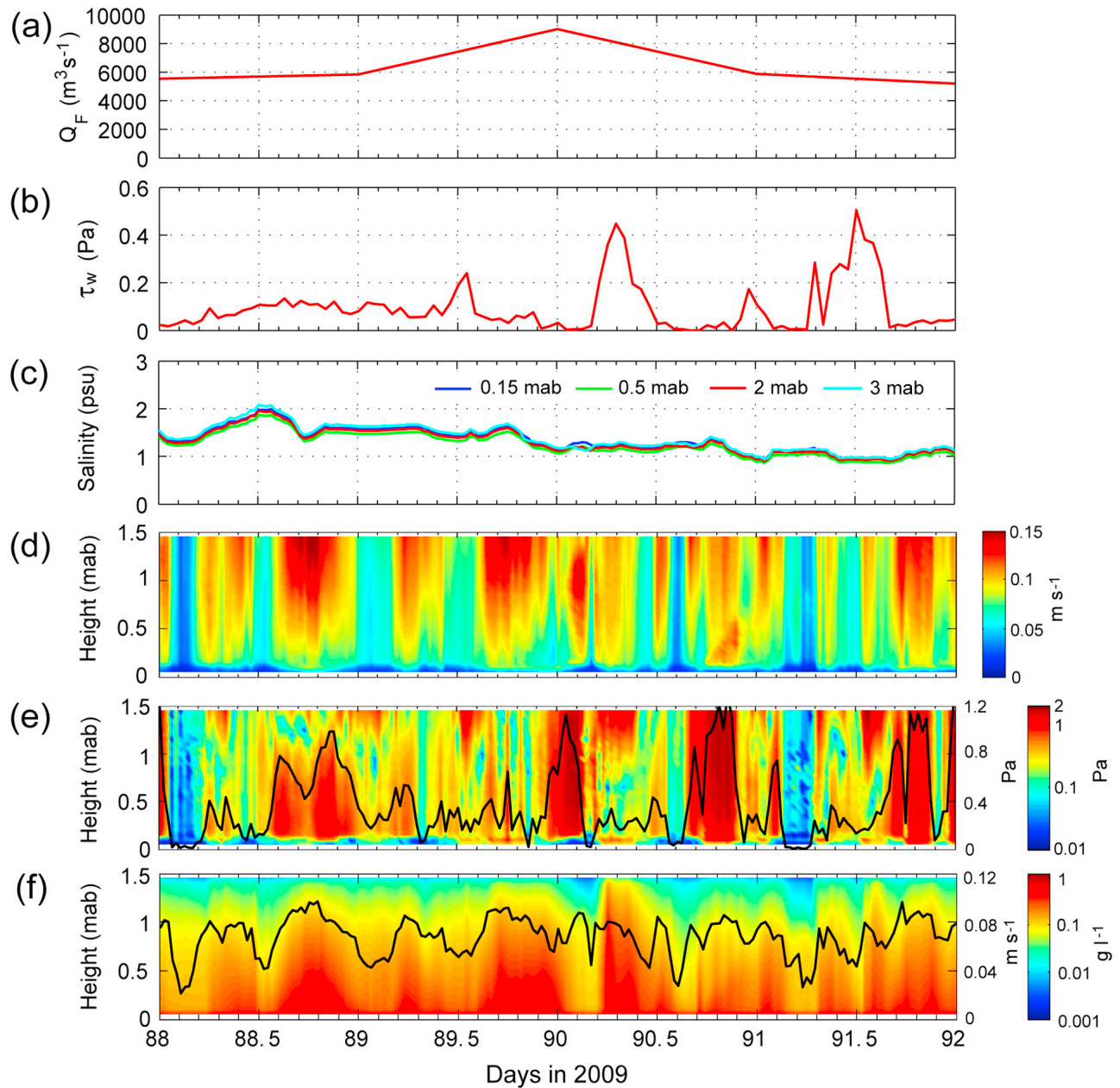


**Figure 6.** Conditions during an extreme flooding event (see Figure 3a): (a) freshwater discharge, (b) wind stress, (c) salinities at four levels, (d) current speed, (e) Reynolds stress, and (f) ADCP-derived SSC. The black solid lines in Figures 6e and 6f are the Reynolds stress at the 27th bin (0.125–0.175 mab) and the BBL-averaged current speed, respectively.

A mirror image of SSC between maximum flood and maximum ebb was found. For instance, the bottom sediment was resuspended up to 0.7 mab on 330.7 d (maximum flood), gradually settled to form the 0.5-m thick high-concentration layer on 330.9 d, and resuspended again up to 0.8 mab on 331.1 d (maximum ebb). The characteristics of the high-concentration layer were different between SBF and SBE. During the longer SBF, the high-concentration layer was thinner and short lasted, which was quickly resuspended at the onset of tidal acceleration. During the shorter SBE, the high-concentration layer lasted longer with a thicker thickness of about 0.5 m.

#### 4.2. Wind Forcing

[24] In order to address the bottom sediment response to strong wind forcing, the most energetic storm period with  $\tau_w > 0.1$  Pa lasting for 34 h ( $S_3$  in Figure 2b) was examined in Figure 5. This storm occurred during equatorial tide with low freshwater discharge (mean  $Q_F = 261 \text{ m}^3 \text{ s}^{-1}$ ), and thus is ideal to show the dramatic changes before and after the storm passage.

[25] The salinity at 0.15 mab was almost identical to that at 0.5 mab, whereas relatively strong stratification still existed between 0.5 and 1 mab (Figure 5b). When strong

$\tau_w$  was applied, the salinities abruptly decreased by 3–4 psu at all levels. Stratification between 0.5 and 1 mab not only survived but became even stronger after the storm passage. The strong  $\tau_w$  with a peak close to 0.6 Pa was not able to fully mix the BBL, and the salinity at 1 mab decreased more than that at 0.5 mab, resulting in a stronger stratification after the storm passage. The maximum current increased up to  $0.23 \text{ m s}^{-1}$  at 1.41 mab on 325 d (Figure 5c). As the  $\tau_w$  exceeded 0.1 Pa, the increase in current speed started in the upper BBL, and then propagated down to the lower BBL. The current speed of the near-bed 0.5-m layer was not affected as much as the water above.

[26] The  $\tau_R$  increased sharply, reaching its maximum of 0.95 Pa on 324.9 d (Figure 5d). Before the storm, the SSC remained at the background level ( $0.015\text{--}0.03 \text{ g l}^{-1}$ ). As the storm approached, strong mixing-induced resuspension of bottom sediment increased the SSC, resulting in the maximum SSC of  $0.33 \text{ g l}^{-1}$  on 325.2 d (Figure 5e). The high SSC in BBL did not last long, and SSC started to decrease on 325.5 d, likely due to settling. The BBL-averaged current speed slightly reduced on 325.5 d, which might have provided a favorable condition for settling and deposition. On 326 d, meanwhile, the deposited sediment was resuspended by the increased current speed and  $\tau_R$  (Figures 5d and 5e). After the storm passage, the SSC returned to the background level, and it took about 6.8 h (average for six wind events of  $S_1$  to  $S_6$ ) after the  $\tau_w$  decreased below a critical value for erosion (see section 5.2).

### 4.3. Freshwater Discharge

[27] In order to investigate the role of freshwater discharge in controlling SSC, an extreme flooding event with a peak discharge  $>9000 \text{ m}^3 \text{ s}^{-1}$  (88–92 d in Figure 3a) was examined in Figure 6. The maximum freshwater discharge during this period was  $9011 \text{ m}^3 \text{ s}^{-1}$ , corresponding to nearly 5-year-recurrence flood event [Schroeder, 1977]. This time window, corresponding to tropic tide, had several strong wind events (Figure 6b) but the prevailing direction was not always northerly, unlike in the 2008 winter survey. It is noted, therefore, that not all observed signals could be attributable to the flooding freshwater discharge.

[28] The salinities at all measured levels were almost fresh ( $<2$  psu). A huge freshwater discharge pushed the saline water seaward throughout the entire water column in this shallow part of Mobile Bay. As a result, the salinity difference between near-surface (3 mab) and near-bottom (0.15 mab) was negligibly small, indicating that the water column was fully mixed (Figure 6c). No tidal signal was found on salinity. The fully-mixed condition persisted throughout the 2009 spring survey (not shown). The current speed was stronger and the duration was longer during ebb than during flood before the extreme flooding event on 90 d (Figure 6d). The tidal signal on current speed and  $\tau_R$  no longer existed while being influenced by the extreme flooding event.

[29] During this time period, the near-bed SSC was quite high (Figure 6f). On 90.25 d, for example, the near-bed SSC increased up to  $1.11 \text{ g l}^{-1}$  at 0.15 mab. Noticeably, this SSC associated with a peak  $\tau_w$  of 0.42 Pa was much higher than the maximum near-bed SSC associated with a stronger  $\tau_w$  of 0.59 Pa during the storm event in 2008 (Figure 5e). This observation indicates that the sediment bed during the spring

flooding period in 2009 had more sediment available for erosion/resuspension than the stormy winter period in 2008.

## 5. Discussion

### 5.1. Effect of Tides

[30] Under fair weather conditions, the SSC showed a small, abrupt increase at the initiation of tidal acceleration (e.g., 330.4 d), but it did not last long (Figure 4). The SSC started to rapidly increase again on 330.6 d. The same pattern was repeated at the following tidal cycles (e.g., 331.4–331.6 d and 332.35–332.5 d). This pattern can be explained by the re-dispersion process proposed in *Ha and Maa* [2009]. A small amount of fluffy sediments newly deposited during the previous slack tide can be easily agitated and re-dispersed because a sufficient time has not been elapsed for consolidation and thus the erosion threshold is negligibly small or nearly zero [Maa and Kim, 2001]. Also, they tend to be quickly re-deposited when the bed shear stress falls below a critical shear stress for deposition [Ha and Maa, 2009].

[31] Under fair weather conditions with calm wind and low freshwater discharge, the SSC started to decrease even before the BBL-averaged current speed reached its maximum (Figure 4e). This behavior that erosion/resuspension has reduced or ceased by the time the bed shear stress reached its maximum is indicative of type-I (depth-limited) erosion that has been observed in other systems [Sanford and Maa, 2001; Aberle et al., 2004]. In the shallow part of Mobile Bay, erosion may be limited by the limited amount of unconsolidated bed sediment available for erosion only during periods of relatively low freshwater discharge with little sediment supply.

[32] Most previous studies in the micro-tidal estuaries assumed that the tidally-driven contribution to SSC variation in BBL might be negligible. In the micro-tidal estuaries along NGOM, e.g., Galveston Bay, it is also claimed that the sediment resuspension is heavily influenced by the meteorologically driven shear stress rather than tidally driven shear stress [Dellapenna et al., 2006]. This study, however, supports that, at least in the shallow part of Mobile Bay, tidal forcing may play a noticeable role in the cyclic sediment erosion and deposition in BBL (Figure 4). The currents during tropic tides were strong enough to produce the near-bed high-concentration layer, but not strong enough to fully break up the relatively strong stratification in BBL. The duration and thickness of the high-concentration layer also showed tidal characteristics. The longer SBF provided a sufficient time for settling and deposition of suspended sediment, resulting in the thinner, shorter-lasting high-concentration layer, which was quickly resuspended at the onset of tidal acceleration. The shorter SBE resulted in the high-concentration layer that was thicker and lasted longer.

### 5.2. Effect of Wind and Freshwater Discharge

[33] During the winter stormy season, the background SSC was low ( $0.015\text{--}0.03 \text{ g l}^{-1}$ ) probably because the low freshwater discharge delivered less river-borne sediment. An episodic storm was a major forcing, and was strongly associated with the short-lasting high SSC peak in BBL (Figure 2). The variation in SSC in response to wind stress showed that the BBL-averaged SSC remained at the background level during weak wind forcing (Figure 7a). As the

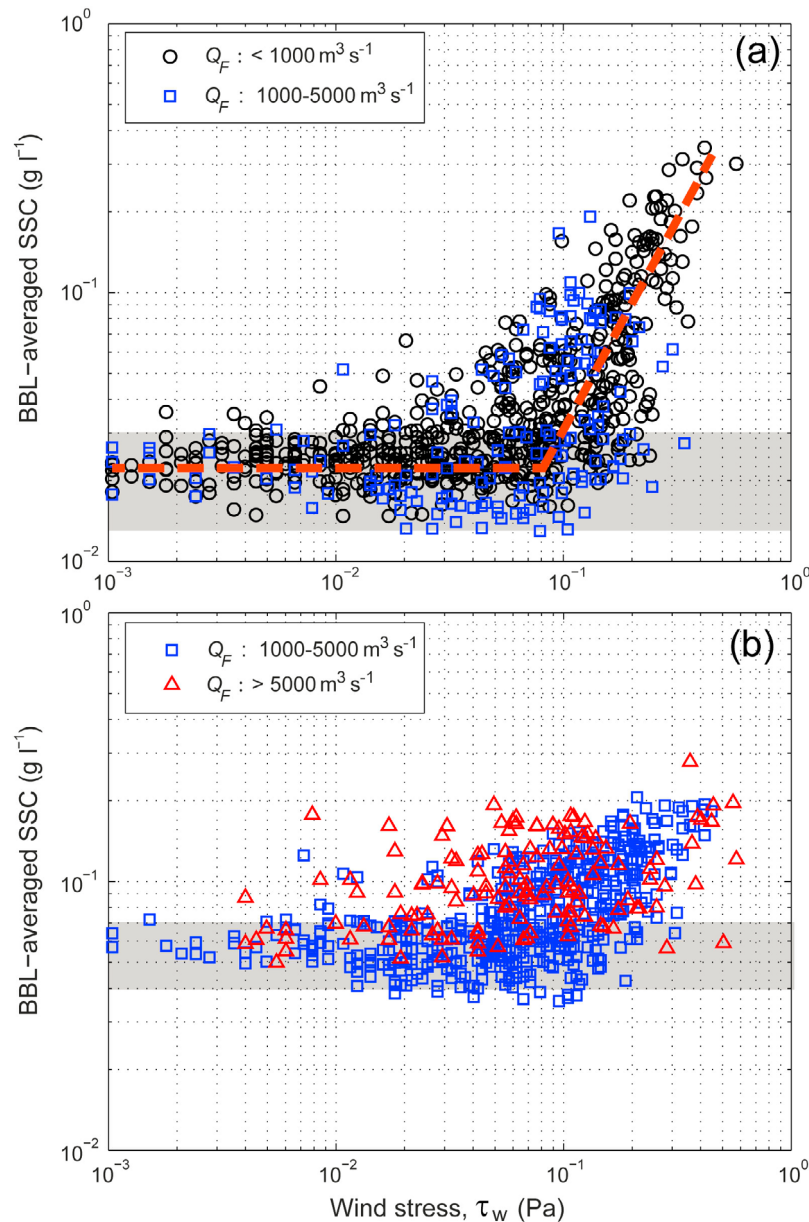


**Figure 7.** Response of the BBL-averaged SSC to wind stress: (a) winter 2008 and (b) spring 2009. The dashed line in Figure 7a indicates the interpreted line ( $R = 0.67$  for  $\tau_w > 0.08$  Pa) to define a critical wind stress for erosion, and the shaded areas in Figures 7a and 7b represent the respective background concentrations. Note that the effect of wind forcing on SSC is not clear for high discharge condition ( $Q_F > 5000 \text{ m}^3 \text{ s}^{-1}$ ).

$\tau_w$  exceeded 0.08–0.1 Pa, SSC started to rapidly increase, indicating the presence of a critical wind stress for erosion. When the wind stress was larger than 0.8 Pa the SSC was correlated with wind stress ( $R = 0.67$ ).

[34] During the spring flooding period, on the other hand, the background SSC was relatively high (0.04–0.07  $\text{g l}^{-1}$ ) likely due to the large sediment supply from high freshwater discharge and bed softening leading to easier sediment erodibility. In spring 2009, when freshwater discharge was  $< 5000 \text{ m}^3 \text{ s}^{-1}$ , a critical wind stress of 0.08–0.1 Pa still existed, but for high discharge condition ( $> 5000 \text{ m}^3 \text{ s}^{-1}$ ), it is difficult to define a critical wind stress for erosion and SSC was no longer a function of wind stress (Figure 7b).

This indicates that the wind-induced erosion/resuspension was not able to enhance the already high SSC in BBL during the spring flooding period. The correlation ( $R = 0.78$ ) between wind stress and SSC during the low discharge period ( $< 1000 \text{ m}^3 \text{ s}^{-1}$ ) was higher than that ( $R = 0.56$ ) during the high discharge period ( $> 5000 \text{ m}^3 \text{ s}^{-1}$ ). This suggests that the wind mixing could effectively transfer the momentum to generate the high-concentration suspension of sediment during the low discharge period when the wind mixing capacity tends to be strong. During the high discharge period, the freshwater discharge becomes the more important controlling factor that can maintain the sediment in suspension, regardless of the strength of wind forcing.

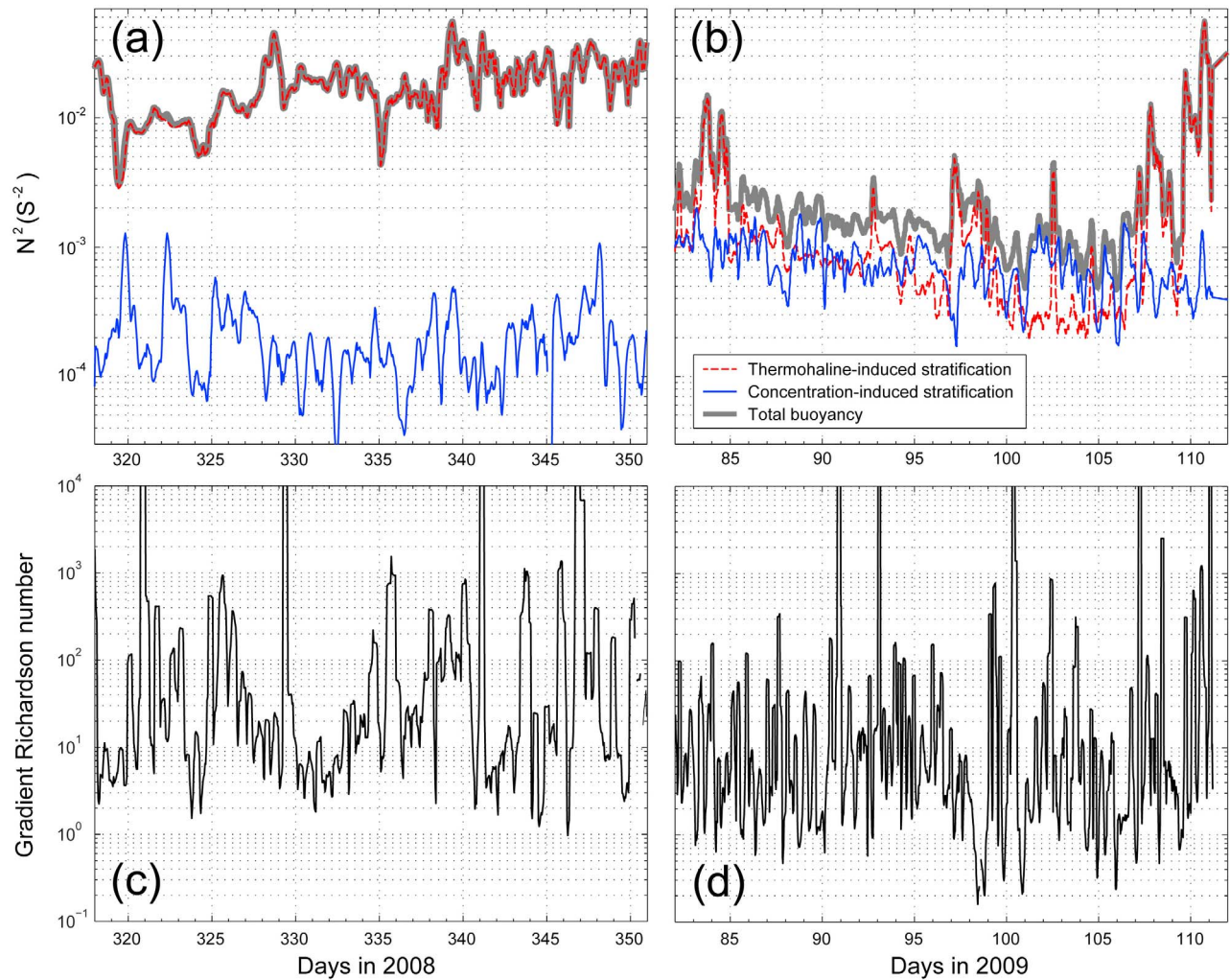


**Figure 8.** Comparison between two contrasting seasons: thermohaline-induced and concentration-induced stratification in (a) winter 2008 and (b) spring 2009 and gradient Richardson numbers in (c) winter 2008 and (d) spring 2009. The 6-h moving average was applied to reduce noises.

### 5.3. Effect of Stratification

[35] In a turbid, highly-stratified estuarine system such as Mobile Bay, it is meaningful to assess the role of stratification in controlling the sediment resuspension in BBL. Stratification stabilizes the water column and may suppress mixing when it overcomes shear instability. The relative importance of stratification-induced stability and velocity shear-induced instability is expressed by the gradient Richardson number ( $Ri$ ). In a sediment-laden boundary layer,  $Ri$  is defined as

$$N^2 = -\frac{g}{\rho} \frac{d\rho}{dz} = -\frac{g(\rho_s - \rho)}{\rho} \frac{dC}{dz} - \frac{g}{\rho} \frac{d\sigma}{dz}, \quad (4a)$$

$$Ri = \left( \frac{N}{du/dz} \right)^2, \quad (4b)$$

where  $N$  is buoyancy frequency,  $u$  is current velocity,  $g$  is gravitational acceleration,  $\rho_s$  and  $\rho$  are sediment and water densities, respectively,  $C$  is sediment volume concentration,

$\sigma$  is thermohaline density anomaly, and  $z$  is distance above the bed [Wright *et al.*, 1999; Friedrichs *et al.*, 2000].

[36] The buoyancy frequency, a measure of stratification, is governed by two contributors (equation (4a)): (1) sediment volume concentration; and (2) thermohaline density anomaly. To examine the competition between these two contributors, ADCP-derived SSCs and densities measured by YSI probes were used. During winter 2008, the buoyancy frequency was almost entirely determined by the thermohaline-induced stratification (Figure 8a). As a whole, the total buoyancy was  $O(10^{-2} \text{ s}^{-2})$ . The contribution of thermohaline density gradient to the buoyancy was about 2 orders of magnitude larger than that of concentration gradient. During spring 2009, on the other hand, the contribution of thermohaline density gradient considerably weakened, but that of concentration gradient strengthened (Figure 8b). The two processes made approximately equal contribution to the total buoyancy of  $O(10^{-3} \text{ s}^{-2})$ , an order of magnitude smaller compared to that during winter 2008. Relatively strong stratification during winter 2008 might limit the transfer of momentum into the BBL, and suppress velocity shear-induced instability. Such stratification

**Table 2.** Distributions of the Gradient Richardson Number,  $Ri$ , Under Different Discharge Conditions

| Freshwater Discharge ( $Q_F$ )                 | $Ri < 1$ | $Ri > 1$ |
|--|----------|----------|
| $<1000 \text{ m}^3 \text{ s}^{-1}$             | 4.8%     | 95.2%    |
| $1000\text{--}5000 \text{ m}^3 \text{ s}^{-1}$ | 25.0%    | 75.0%    |
| $>5000 \text{ m}^3 \text{ s}^{-1}$             | 23.6%    | 76.4%    |

may enhance the accumulation of suspended sediment near the bed by dampening turbulence, which can lead to the formation of a thick high-concentration layer in BBL [Adams and Weatherly, 1981; Stumpf *et al.*, 1993; Friedrichs *et al.*, 2000]. Schroeder and Wiseman [1986] claimed that the strong stratification in Mobile Bay could frequently occur in the condition of both low freshwater discharge and persistent southward-directed wind stress, due to a relatively weak tidal forcing and a small bay volume ( $3.2 \times 10^9 \text{ m}^3$  [Environmental Protection Agency, 1989]) relative to tremendous freshwater input.

[37] The  $Ri$  was estimated using equation (4b) for BBL to examine the relative importance between stratification and shear instability (Figures 8c and 8d). Large values of  $Ri$  indicate a stable condition, while low values may indicate dynamic instability, with the transition taking place at a critical Richardson number of order of one [van Gastel and Pelegri, 2004]. The  $Ri$  showed a noticeable difference between winter 2008 and spring 2009. During winter 2008, the  $Ri$  was mostly  $>1$  (93.9% of the data), indicating that the BBL was strongly stratified, and mixing was likely only during the intermittent storm events. During spring 2009, on the other hand, the  $Ri$  was  $<1$  for 25.7% of the data, indicating that the BBL was less stratified and mixing occurred more frequently. Based on the freshwater discharge conditions, the statistics of  $Ri$  was reanalyzed to examine the role of discharge in determining the likelihood of mixing (Table 2). During the low discharge ( $<1000 \text{ m}^3 \text{ s}^{-1}$ ), the  $Ri$  was  $>1$  for 95.2% of the data, suggesting that the BBL had a unfavorable condition for sediment resuspension due to the strong thermohaline-induced stratification. Noticeably, during the moderate discharge ( $1000\text{--}5000 \text{ m}^3 \text{ s}^{-1}$ ), the mixing occurred more frequently with the  $Ri < 1$  for 25.0% of the data. Further increases in freshwater discharge ( $>5000 \text{ m}^3 \text{ s}^{-1}$ ) did not change the mixing regime. These distributions of  $Ri$  indicate that the relatively low freshwater discharge yielded a stable, stratified condition, and that the moderate-to-flooding discharge pushed the saline water seaward to form a destratified condition throughout the water column. Such destratification favored the turbulent mixing, facilitating the upward transport of high SSC water trapped near the bed.

#### 5.4. Limitations

[38] Given the limitations of the data set, there are a few issues that this study is not able to address. The main issue is a lack of wind wave data. It is the combined bed shear stress of currents and waves that controls sediment erosion/resuspension in BBL [Grant and Madsen, 1986; Wright, 1995; Lee, 2010]. Data for wind waves were not collected in this study. There are only a few publications that address wind waves, excluding storm surges, in Mobile Bay [Chen *et al.*, 2005; Roland and Douglass, 2005], and there is no

journal publication that reports any data or information for wave-induced bed shear stress. With no information available for wave-induced bed shear stress, this study was unable to assess the relative contribution of waves and currents in generating bed shear stress. Instead, therefore, this study tried to relate wind stress to sediment erosion in BBL, showing a good correlation between wind stress and SSC and the presence of a critical wind shear stress of 0.08–0.1 Pa for sediment erosion when freshwater discharge was  $<5000 \text{ m}^3 \text{ s}^{-1}$  (Figure 7).

[39] Another limitation is that this study was based on data from single mooring site. Given the limited observations in Mobile Bay, it is not clear how representative the data from our station are for the entire Bay. The conditions in the deep ship channel are expected to be different, although no time series observations are available because mooring instruments is prohibited in the federally managed ship channel. Compared to the shallow areas, near-bottom currents would be more affected by the stronger gravitational circulation present in the ship channel [Wiseman *et al.*, 1988]. It is likely that surface wind stress would get weaker near the bottom of the deep ship channel. The frequent transition between stratification and destratification as a function of freshwater discharge (Figure 8) is likely to be confined to the shallow areas because the strong vertical density gradient persists along the deep ship channel throughout the year [Dzwonkowski *et al.*, 2011]. The effect of some forcing conditions may also vary along the estuary. Observations in the shallow inner part of Mobile Bay [Park *et al.*, 2007a], for example, show much weaker tidal signal in current velocity compared to that in this study. Relatively strong wind conditions tend to be uniform over the entire Bay, and thus the conclusions for the wind-dominated period are expected to be applicable throughout the shallow parts of the Bay. The effect of freshwater discharge seems to vary along the estuary, with river influence mostly confined to the northern portion of the Bay [Schroeder and Wiseman, 1986; Kim and Park, 2012].

## 6. Conclusions

[40] The sediment behavior in BBL of Mobile Bay is controlled by several forcing mechanisms. The most favorable forcing for sediment resuspension is the combined condition of strong wind, tropic tide and moderate-to-high freshwater discharge. Mooring measurements at two contrasting seasons showed different typical sediment behavior.

[41] In winter, Mobile Bay predominantly experiencing northerly wind and low freshwater discharge showed relatively low background SSC. Local resuspension by the episodic storm events, despite the persistent stratification outside of the near-bed 0.5-m layer, was responsible for the intermittent, short-lasting high SSC in BBL. In spring, Mobile Bay predominantly experiencing southerly wind and high freshwater discharge showed relatively high background SSC (2–3 times of winter season background level). The high concentration during flood events was likely due to the large amount of suspended sediment from the fluvial input and bed softening leading to easier sediment erodibility. They can play an important role in forming a high-concentration layer near the bed which can be readily resuspended into the overlying well-mixed water column.

[42] Despite a micro-tidal regime, probably due to the shallow depth of Mobile Bay, tidal currents produced distinct variations in salinity and velocity during tropic tides, resulting in noticeable signatures of erosion and deposition in BBL. When freshwater discharge was  $<5000 \text{ m}^3 \text{ s}^{-1}$ , a good correlation existed between wind stress and SSC, showing the presence of a critical wind stress of  $0.08\text{--}0.1 \text{ Pa}$ . When freshwater discharge was  $>5000 \text{ m}^3 \text{ s}^{-1}$ , wind stress was no longer a main controller for SSC, showing a relatively poor correlation between the two. During the low-energy period with low freshwater discharge, the near-bed thermohaline density anomaly was a major factor that determined the stratification in BBL. When the Mobile River system provided a large freshwater discharge, the entire water column in shallow areas was mostly influenced by freshwater input, so that the thermohaline anomaly's contribution to the stratification considerably weakened while the SSC's contribution strengthened.

[43] **Acknowledgments.** We thank the DISL's Tech Support Group including K. Weis, N. Nazarian, A. Gunter and L. Linn for their assistance in the field and laboratory. This study was supported by the Gulf of Mexico Research Initiative (GoMRI) Rapid Response and the NSF Northern Gulf Coastal Hazards Collaboratory (award EPS-1010607). In the developing stage of acoustic inversion algorithm, H.K. Ha was supported by KOPRI grant (PE10260).

## References

- Aberle, J., V. Nikora, and R. Walters (2004), Effects of bed material properties on cohesive sediment erosion, *Mar. Geol.*, *207*, 83–93, doi:10.1016/j.margeo.2004.03.012.
- Adams, C. E., and G. L. Weatherly (1981), Some effects of suspended sediment stratification on an oceanic bottom boundary layer, *J. Geophys. Res.*, *86*(C5), 4161–4172, doi:10.1029/JC086iC05p04161.
- Chen, Q., H. Zhao, K. Hu, and S. L. Douglass (2005), Prediction of wind waves in a shallow estuary, *J. Waterw. Port Coastal Ocean Eng.*, *131*, 137–148, doi:10.1061/(ASCE)0733-950X(2005)131:4(137).
- Deines, K. L. (1999), Backscatter estimation using broadband acoustic Doppler current profilers, in *Proceedings of the IEEE Sixth Working Conference on Current Measurement*, pp. 249–253, Inst. Electr. and Electron. Eng., New York.
- de Jonge, V. N., and J. E. E. van Beusekom (1995), Wind- and tide-induced resuspension of sediment and microphytobenthos from tidal flats in the Ems Estuary, *Limnol. Oceanogr.*, *40*, 776–778, doi:10.4319/l.1995.40.4.0776.
- Dellapenna, T. M., M. A. Allison, G. A. Gill, R. D. Lehman, and K. W. Warnken (2006), The impact of shrimp trawling and associated sediment resuspension in mud dominated, shallow estuaries, *Estuarine Coastal Shelf Sci.*, *69*, 519–530, doi:10.1016/j.ecss.2006.04.024.
- Downing, J. (2006), Twenty-five years with OBS sensors: The good, the bad, and the ugly, *Cont. Shelf Res.*, *26*, 2299–2318, doi:10.1016/j.csr.2006.07.018.
- Dzwonkowski, B., K. Park, H. K. Ha, W. M. Graham, F. J. Hernandez, and S. P. Powers (2011), Hydrographic variability on a coastal shelf directly influenced by estuarine outflow, *Cont. Shelf Res.*, *31*, 939–950, doi:10.1016/j.csr.2011.03.001.
- Environmental Protection Agency (1989), Strategic assessment of near coastal waters: Northeast case study. *Susceptibility and Status of Gulf of Mexico Estuaries to Nutrient Discharge: Summary Report, Part 3*, Strategic Assessment Branch, Natl. Oceanic and Atmos. Admin., Rockville, Md.
- Friedrichs, C. T., L. D. Wright, D. A. Hepworth, and S.-C. Kim (2000), Bottom-boundary-layer processes associated with fine sediment accumulation in coastal seas and bays, *Cont. Shelf Res.*, *20*, 807–841, doi:10.1016/S0278-4343(00)00003-0.
- Gordon, R. L. (Ed.) (1996), Acoustic Doppler current profiler: Principle of operation a practical primer, report, 57 pp., RD Instrum., San Diego, Calif.
- Grant, W. D., and O. S. Madsen (1986), The continental shelf bottom boundary layer, *Annu. Rev. Fluid Mech.*, *18*, 265–305, doi:10.1146/annurev.fl.18.010186.001405.
- Ha, H. K., and J. P.-Y. Maa (2009), Evaluation of two conflicting paradigms for cohesive sediment deposition, *Mar. Geol.*, *265*, 120–129, doi:10.1016/j.margeo.2009.07.001.
- Ha, H. K., J. P.-Y. Maa, K. Park, and Y. H. Kim (2011), Estimation of high-resolution sediment concentration profiles in bottom boundary layer using pulse-coherent acoustic Doppler current profilers, *Mar. Geol.*, *279*, 199–209, doi:10.1016/j.margeo.2010.11.002.
- Hoitink, A. J. F., and P. Hoekstra (2005), Observations of suspended sediment from ADCP and OBS measurements in a mud-dominated environment, *Coastal Eng.*, *52*, 103–118, doi:10.1016/j.coastaleng.2004.09.005.
- Jay, D. A., and J. D. Musiak (1994), Particle trapping in estuarine tidal flows, *J. Geophys. Res.*, *99*, 20,445–20,461, doi:10.1029/94JC00971.
- Johnson, G. C., R. E. Kidd, C. A. Journey, H. Zappia, and J. B. Atkins (2002), Environmental setting and water quality issues of the Mobile River basin, Alabama, Georgia, Mississippi, and Tennessee., *Water Resour. Invest. Rep. 02-4162*, 62 pp., U.S. Geological Survey, Reston, Va.
- Kim, C.-K., and K. Park (2012), A modeling study of water and salt exchange for a micro-tidal, stratified northern Gulf of Mexico estuary, *J. Mar. Syst.*, *96-97*, 103–115, doi:10.1016/j.jmarsys.2012.02.008.
- Kim, Y. H., and G. Voulgaris (2003), Estimation of suspended sediment concentration in estuarine environments using acoustic backscatter from an ADCP, in *Coastal Sediments 2003*, edited by R. A. Davis, A. Sallenger, and P. Howd, pp. 1–10, World Sci., Hackensack, N. J.
- Kineke, G. C., and R. W. Sternberg (1992), Measurements of high concentration suspended sediments using the optical backscatter sensor, *Mar. Geol.*, *108*, 253–258, doi:10.1016/0025-3227(92)90199-R.
- Lacy, J. R., and C. R. Sherwood (2004), Accuracy of a pulse-coherent acoustic Doppler profiler in a wave-dominated flow, *J. Atmos. Oceanic Technol.*, *21*, 1448–1461, doi:10.1175/1520-0426(2004)021<1448:AOAPAD>2.0.CO;2.
- Lee, H. J. (2010), Preliminary results on suspended sediment transport by tidal currents in Gomsu Bay, Korea, *Ocean Sci. J.*, *45*(3), 187–195, doi:10.1007/s12601-010-0017-0.
- Lohrenz, S. E., G. L. Fahnenstiel, D. G. Redalje, G. A. Lang, M. J. Dagg, T. E. Whitledge, and Q. Dortch (1999), Nutrients, irradiance and mixing as factors regulating primary production in coastal waters impacted by the Mississippi River plume, *Cont. Shelf Res.*, *19*, 1113–1141, doi:10.1016/S0278-4343(99)00012-6.
- Lohrmann, A., B. Hackett, and L. P. Roed (1990), High resolution measurements of turbulence, velocity and stress using a pulse-to-pulse coherent sonar, *J. Atmos. Oceanic Technol.*, *7*, 19–37, doi:10.1175/1520-0426(1990)007<0019:HRMOTV>2.0.CO;2.
- Maa, J. P.-Y., and S.-C. Kim (2001), A constant erosion rate model for fine sediment in the York River, Virginia, *Environ. Fluid Mech.*, *1*, 345–360, doi:10.1023/A:1015799926777.
- MacIntyre, H. L., and J. J. Cullen (1996), Primary production by suspended and benthic microalgae in a turbid estuary: Time-scales of variability in San Antonio Bay, Texas, *Mar. Ecol. Prog. Ser.*, *145*, 245–268, doi:10.3354/meps145245.
- Menon, M. G., R. J. Gibbs, and A. Phillips (1998), Accumulation of muds and metals in the Hudson River estuary turbidity maximum, *Environ. Geol.*, *34*, 214–222, doi:10.1007/s002540050273.
- Mobile Bay National Estuary Program (MBNEP) (2008), State of Mobile Bay: A status report on Alabama's coastline from the delta to our coastal waters, report, 46 pp., Mobile, Ala.
- Noble, M. A., W. W. Schroeder, W. J. Wiseman, H. F. Ryan, and G. Gelfenbaum (1996), Subtidal circulation patterns in a shallow, highly stratified estuary: Mobile Bay, Alabama, *J. Geophys. Res.*, *101*(C11), 25,689–25,703, doi:10.1029/96JC02506.
- Park, K., C. K. Kim, and W. W. Schroeder (2007a), Temporal variability in summertime bottom hypoxia in shallow areas of Mobile Bay, Alabama, *Estuaries Coasts*, *30*(1), 54–65.
- Park, K., J. F. Valentine, S. Sklenar, K. R. Weis, and M. R. Dardeau (2007b), The effects of Hurricane Ivan in the inner part of Mobile Bay, Alabama, *J. Coastal Res.*, *23*(5), 1332–1336, doi:10.2112/06-0686.1.
- Pinckney, J. L., and A. R. Lee (2008), Spatiotemporal patterns of subtidal benthic microalgal biomass and community composition in Galveston Bay, Texas, USA, *Estuaries Coasts*, *31*, 444–454, doi:10.1007/s12237-007-9020-9.
- RD Instruments (2002), High resolution water profiling mode 11, *Field Serv. Appl. Note FSA-013*, 6 pp., San Diego, Calif.
- RD Instruments (2008), ADCP coordinate transformation: Formulas and calculations, *RD Instrum. Tech. Rep. P/N 951-6079-00*, 31 pp., San Diego, Calif.
- Roland, R. M., and S. L. Douglass (2005), Estimating wave tolerance of *Spartina alterniflora* in coastal Alabama, *J. Coastal Res.*, *21*(3), 453–463, doi:10.2112/03-0079.1.
- Sanford, L. P., and J. P.-Y. Maa (2001), A unified erosion formulation for fine sediments, *Mar. Geol.*, *179*, 9–23, doi:10.1016/S0025-3227(01)00201-8.
- Sanford, L. P., S. E. Suttles, and J. P. Halka (2001), Reconsidering the physics of the Chesapeake Bay estuarine turbidity maximum, *Estuaries*, *24*, 655–669, doi:10.2307/1352874.

- Schroeder, W. W. (1977), The impact of the 1973 flooding of the Mobile River system on the hydrography of Mobile Bay and east Mississippi Sound, *Northeast Gulf Sci.*, 1, 68–76.
- Schroeder, W. W. (1979), The dissolved oxygen puzzle of the Mobile Estuary, in *Proceeding of Symposium on the National Resources of the Mobile Estuary, Alabama*, edited by H. A. Loyacano and J. P. Smith, pp. 25–30, Mobile Dist., U.S. Army Corps of Eng., Mobile, Ala.
- Schroeder, W. W., and W. J. Wiseman (1986), Low frequency shelf-estuarine exchange processes in Mobile Bay and other estuarine systems on the northern Gulf of Mexico, in *Estuarine Variability*, edited by D. A. Wolfe, pp. 355–366, Academic, New York.
- Schroeder, W. W., and W. J. Wiseman (1999), Geology and hydrodynamics of Gulf of Mexico estuaries, in *Biogeochemistry of Gulf of Mexico Estuaries*, edited by T. S. Bianchi, J. R. Pennock, and R. R. Twilley, pp. 3–28, John Wiley, New York.
- Shaffer, G. P., and M. J. Sullivan (1988), Water column productivity attributable to displaced benthic diatoms in well-mixed shallow estuaries, *J. Phycol.*, 24, 132–140.
- Stacey, M. T., S. G. Monismith, and J. R. Buran (1999), Measurements of Reynolds stress profiles in unstratified tidal flow, *J. Geophys. Res.*, 104(C5), 10,933–10,949, doi:10.1029/1998JC900095.
- Stumpf, R. P., G. Gelfenbaum, and J. R. Pennock (1993), Wind and tidal forcings of a buoyant plume, Mobile Bay, Alabama, *Cont. Shelf Res.*, 13(11), 1281–1301, doi:10.1016/0278-4343(93)90053-Z.
- Stutes, A. L., J. Cebrian, and A. A. Corcoran (2006), Effects of nutrient enrichment and shading on sediment primary production and metabolism in eutrophic estuaries, *Mar. Ecol. Prog. Ser.*, 312, 29–43, doi:10.3354/meps312029.
- Sutherland, T. F., P. M. Lane, C. L. Amos, and J. Downing (2000), The calibration of optical backscatter sensors for suspended sediment of varying darkness levels, *Mar. Geol.*, 162, 587–597, doi:10.1016/S0025-3227(99)00080-8.
- Thorne, P. D., and D. M. Hanes (2002), A review of acoustic measurement of small-scale sediment processes, *Cont. Shelf Res.*, 22(4), 603–632, doi:10.1016/S0278-4343(01)00101-7.
- Traykovski, P., P. L. Wiberg, and W. R. Geyer (2007), Observations and modeling of wave-supported sediment gravity flows on the Po prodelta and comparison to prior observations from the Eel shelf, *Cont. Shelf Res.*, 27, 375–399, doi:10.1016/j.csr.2005.07.008.
- van Gastel, P., and J. L. Pelegri (2004), Estimates of gradient Richardson numbers from vertically smoothed data in the Gulf Stream region, *Sci. Mar.*, 68(4), 459–482.
- Wainright, S. C., and C. S. Hopkinson Jr. (1997), Effects of sediment resuspension on organic matter processing in coastal environments: A simulation model, *J. Mar. Syst.*, 11, 353–368, doi:10.1016/S0924-7963(96)00130-3.
- Winterwerp, J. C., and W. G. M. van Kesteren (2004), *Introduction to the Physics of Cohesive Sediment in the Marine Environment*, 466 pp., Elsevier, Amsterdam.
- Wiseman, W. J., Jr., W. W. Schroeder, and S. P. Dinnel (1988), Shelf-estuarine water exchanges between the Gulf of Mexico and Mobile Bay, Alabama, *Am. Fish. Soc. Symp.*, 3, 1–8.
- Wren, D. G., B. D. Barkdoll, R. A. Kuhnle, and R. W. Darrow (2000), Field techniques for suspended-sediment measurement, *J. Hydraul. Eng.*, 126, 97–104, doi:10.1061/(ASCE)0733-9429(2000)126:2(97).
- Wright, L. D. (1995), *Morphodynamics of Inner Continental Shelves*, 242 pp., CRC Press, Boca Raton, Fla.
- Wright, L. D., S.-C. Kim, and C. T. Friedrichs (1999), Across-shelf variations in bed roughness, bed stress and sediment suspension on the northern California shelf, *Mar. Geol.*, 154, 99–115, doi:10.1016/S0025-3227(98)00106-6.
- Wu, J. (1980), Wind-stress coefficients over sea surface near neutral conditions- a revisit, *J. Phys. Oceanogr.*, 10, 727–740, doi:10.1175/1520-0485(1980)010<0727:WSCOSS>2.0.CO;2.
- Zhao, H., and Q. Chen (2008), Characteristics of extreme meteorological forcing and water levels in Mobile Bay, Alabama, *Estuaries Coasts*, 31(4), 704–718, doi:10.1007/s12237-008-9062-7.
- Zhao, H., Q. Chen, N. D. Walker, Q. Zheng, and L. H. MacIntyre (2011), A study of sediment transport in a shallow estuary using MODIS imagery and particle tracking simulation, *Int. J. Remote Sens.*, 32, 6653–6671, doi:10.1080/01431161.2010.512938.